

Decimation studies of Bloch electrons in a magnetic field: Higher-order limit cycles underlying the phase diagram

Jukka A. Ketoja,* Indubala I. Satija,† and Juan Carlos Chaves

Department of Physics and Institute of Computational Sciences and Informatics, George Mason University, Fairfax, Virginia 22030

(Received 28 November 1994; revised manuscript received 7 March 1995)

A decimation method is applied to the tight binding model describing the two-dimensional electron gas with next-nearest-neighbor interaction in the presence of an inverse golden mean magnetic flux. The critical phase with fractal spectrum and wave function exists in a finite window in two-dimensional parameter space introducing universal features. Our decimation scheme identifies new quantitative universality classes characterized by the limit cycles of the decimation equations. The limit cycles describe the self-similarity of the wave functions and divide them into three broader qualitative classes where the wave functions are either symmetric, asymmetric, or exhibit a type of shifted symmetry. We conjecture that the rest of the critical phase, where the fractal wave functions do not exhibit self-similarity, is characterized by strange attractors of the renormalization equations. The results are compared with those of Han *et al.* [Phys. Rev. B **50**, 11365 (1994)] on the same model.

The two-dimensional electron gas with irrational magnetic flux is a well-known paradigm in the study of systems with two competing periodicities. The magnetic field results in reducing the problem to a one-dimensional tight binding model¹ (TBM) known as the Harper equation.² The Harper equation exhibits both extended (*E*) and localized (*L*) states. At the onset of transition corresponding to a periodic potential with square symmetry, the states are critical (*C*) with fractal spectra and wave functions. The scaling properties of the devil staircase spectra and the wave functions have been studied extensively using various renormalization group (RG) methods.³⁻⁵

The Harper equation describes not only the Bloch electron problem but also the isotropic *XY* quantum spin model in a modulating magnetic field which is incommensurate with respect to the lattice. Recently, it was shown that the presence of anisotropy in spin space fattened the critical point of the Harper equation resulting in a phase diagram where *E*, *L*, and *C* phases all existed in a finite parameter interval.⁶ The existence of a fat *C* phase provided a new scenario for the breakdown of analyticity in incommensurate systems. Furthermore, based on numerical results obtained using a new decimation method,^{5,7} it was argued that the fat *C* phase was described by four distinct universality classes characterized by limit cycles of the RG flow.

Very recently, the fat *C* phase was reported also in the original Bloch electron context by Han *et al.*⁸ The *C* phase was observed considering Bloch electrons on a square lattice where the coupling t_{ab} to next-nearest-neighbor (NNN) sites exceeded a certain threshold value compared to the nearest-neighbor (NN) couplings t_a and t_b . The associated TBM has the form

$$(t_a + 2t_{ab} \cos\{2\pi[\sigma(i + \frac{1}{2}) + \phi]\})\psi_{i+1} + (t_a + 2t_{ab} \cos\{2\pi[\sigma(i - \frac{1}{2}) + \phi]\})\psi_{i-1} + 2t_b \cos[2\pi(\sigma i + \phi)]\psi_i = E\psi_i, \quad (1)$$

where σ is the magnetic flux. Figure 1 shows the phase

diagram of the model in the two-dimensional space of the parameters $\lambda = \frac{t_b}{t_a}$ and $\alpha = 2\frac{t_{ab}}{t_a}$. The Harper equation corresponds to the limit $\alpha = 0$ where the NNN coupling term is zero. The phase diagram was obtained using analytical methods to obtain the scaling behavior of the total bandwidth (TBW) and the Lyapunov exponents and carrying out a numerical multifractal analysis.⁸ The lines *AC* (*E-C* transition) and *CE* (*C-L* transition) were found to be bicritical; i.e., the TBW scaled with the system size with the exponent $\delta = 2$. This was in contrast with the critical line *BC* separating the *E* and *L* phases

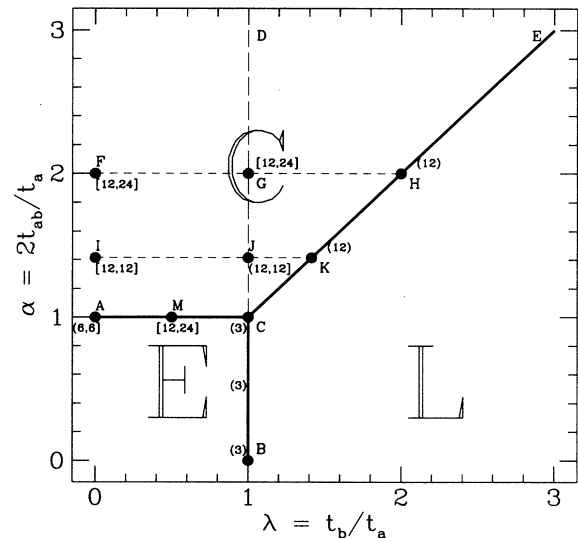


FIG. 1. The phase diagram of the electron gas. The solid lines *BC*, *AC*, and *CE* are respectively the *E-L*, *E-C*, and *C-L* transition lines. The dark solid circles describe the points where decimation equations exhibit limit cycles. With the exception of the point *C*, the *BC* line is described by the Harper universality class. The period of a limit cycle is indicated in a bracket close to the point: (*p*), [*p*], and [*p*] brackets respectively describe symmetric, asymmetric, and shifted symmetry cycles of period *p*.

where the exponent was known to be unity. Furthermore, oscillatory behavior superposed on the power law dependence showed up in the bicritical case. For the sequence $\sigma = 1/q$ ($q = 1, 2, 3, \dots$) the observed periodicities were understood from a WKB analysis. However, the origin of the regular periodicities for the Fibonacci sequence remained rather unclear although the oscillations were conjectured to be related to the number theoretic properties of the Fibonacci numbers. Within the region bounded by the lines AC and CE and the α axis, where the NNN coupling dominated, the numerical results suggested that the TBW scaled with a noninteger exponent. In this region, the oscillations around the power law were generally irregular except for some special points (e.g., at point G a period 4 was observed). In the multifractal analysis there were complications as well due to a lack of convergence in the $f(\alpha)$ curve with the size of the system. However, this regime was conjectured to be critical.

We apply decimation methods to the TBM given by Eq. (1) with $\sigma = (\sqrt{5} - 1)/2$. Our motivation is to confirm the existence of the critical phase and determine universality classes within this phase. Unlike a previous study⁸ which investigated the scaling properties of the fractal set of *eigenvalues*, we study the scaling properties of the fractal *eigenstates*. Our *exact* decimation equations which take into account the underlying incommensurate frequency σ can be iterated numerically for extremely large system sizes. In this approach, the self-similar wave functions are expected to lead to a limit cycle in the RG equations.⁵ The limit cycles can be used to extract information on the scaling of a wave function and hence they characterize the corresponding universality classes.

Our decimation approach describes the scaling properties of the wave functions for a specific value of energy. In the critical phase, the self-similar behavior is usually observed only for the minimum and maximum energy states and also for the band center if $E = 0$ is an eigenenergy. In our studies below, we will focus on the quantum state corresponding to E_{\min} . In addition to fixing the quantum state, one has to also fix the phase factor ϕ in Eq. (1). It has been pointed out in previous studies^{3,5} that the wave function ψ_i obtained by iterating the TBM diverges unless the phase factor ϕ is tuned to some critical value ϕ_c . In the Harper model, $\phi_c = \frac{1}{2}$ for the negative band edge. For this value, the main peak is centrally located and the wave function is symmetric about $i = 0$. In the study of the quantum spin model,⁵ the phase factor had to be varied continuously in the fat C phase so that the main peak could be centrally located and the resulting wave function became bounded. Determination of ϕ_c was essential in order to find the RG limit cycles and to compute the universal scaling ratios. In general the phase factor ϕ for obtaining a symmetric wave function need not be identical to the phase factor resulting in a bounded wave function.⁵

We consider an infinite lattice which extends in both positive and negative directions from the $i = 0$ site. In the decimation scheme, all sites except those labeled by positive as well as negative Fibonacci numbers are decimated. The resulting TBM connecting the wave function ψ at two neighboring Fibonacci sites can be written as

$$\psi(i + F_{n+1}) = c_n^+(i)\psi(i + F_n) + d_n^+(i)\psi(i), \quad (2)$$

$$\psi(i - F_{n+1}) = c_n^-(i)\psi(i - F_n) + d_n^-(i)\psi(i). \quad (3)$$

The index n above refers to the level of decimation. For the Harper model it suffices to define only one set of the “decimation functions” $c_n(i)$ and $d_n(i)$ because of the symmetry of the bounded wave function about $i = 0$. For the TBM (1) such a symmetry cannot always be found and therefore we have to introduce separate decimation functions for the positive (+) and the negative (−) side.

Using the defining property of the Fibonacci numbers, $F_{n+1} = F_n + F_{n-1}$, the following recursion relations are obtained analytically for c_n and d_n (we will omit the +, − indices if the equations do not depend upon them)^{7,5}:

$$c_{n+1}(i) = c_n(i + F_n)c_{n-1}(i + F_n) - d_n^{-1}(i)d_{n+1}(i),$$

$$d_{n+1}(i) = -d_n(i)[d_n(i + F_n)$$

$$+ c_n(i + F_n)d_{n-1}(i + F_n)]c_n^{-1}(i). \quad (5)$$

For a fixed i , the above coupled equations for the decimation functions define a RG flow which asymptotically ($n \rightarrow \infty$) converge on an attractor. In our earlier studies, the E , C , and L phases were distinguished by distinct attractors of the RG flow. In the Harper as well as in the quantum spin case, the C phase was characterized by a *nontrivial* asymptotic p cycle at the band edges with p equal to 3 or 6. As discussed in our earlier paper,⁵ the conjecture for the existence of limit cycle provides a very efficient Newton method where the energy as well as the cycle can be determined self-consistently to a very high precision.

The existence of a nontrivial p cycle for the decimation functions can be used to define the scaling ratios

$$\zeta_j = \lim_{n \rightarrow \infty} |\psi(F_{pn+j})/\psi(0)|, \quad j = 0, \dots, p-1. \quad (6)$$

This equation describes the decay of the wave function with respect to the central peak and therefore the definition is meaningful only for the critical value of the phase factor ϕ_c leading to a bounded wave function. A well-defined limit ζ_j exists for an integer p for which asymptotically $\psi(F_{n+p}) \approx \psi(F_n)$. The scaling ratios are useful in comparing different universality classes.

By studying the asymptotic behavior of the decimation functions we can confirm the structure of the phase diagram in Fig. 1: For fractal wave functions the associated decimation functions exhibit nontrivial limiting behavior, thereby distinguishing the C states from the E and L states. As summarized in the phase diagram, some of the points in the C phase exhibit limit cycles. For the phase factor $\phi = 1/2$, points B and C were found to exhibit a period-3 limit cycle while for point A the period was 6. On the other hand, we found period 12 for M , F , G , H , I , J , and K . All these limit cycles, obtained with $\phi = 1/2$, resulted in the decimation functions which were equal on the positive and negative side and the corresponding wave functions were symmetrical about $i = 0$.

With the exception of the wave functions at B , C , K , and H , the symmetric wave functions for $\phi = 1/2$ are *unbounded*. However, by tuning the phase factor ϕ to a critical value ϕ_c , bounded wave functions can be obtained as summarized in Fig. 1 and in Table I. It turns out that the bounded wave functions obtained with ϕ_c different from $1/2$ are not symmetric about $i = 0$ and

TABLE I. Special points of the phase diagram and the corresponding parameter values. We also show the cycle length at the critical value ϕ_c of the phase factor and the TBW cycle, which refers to the length of the oscillation in the TBW as obtained from Ref. 8.

	λ	α	ϕ_c	Cycle	TBW cycle
<i>B</i>	1	0	1/2	3	1
<i>C</i>	1	1	1/2	3	1
<i>A</i>	0	1	1/4	6	-
<i>M</i>	1/2	1	0.3202185	24	4
<i>F</i>	0	2	5/18	24	-
<i>G</i>	1	2	1/3	24	4
<i>H</i>	2	2	1/2	12	-
<i>I</i>	0	$\sqrt{2}$	1/4	12	6
<i>J</i>	1	$\sqrt{2}$	3/8	12	6
<i>K</i>	$\sqrt{2}$	$\sqrt{2}$	1/2	12	-

the corresponding decimation functions on the positive and negative side are different. These asymmetric wave functions fall into two different categories. For points *A* and *J*, the wave function is completely asymmetric about $i = 0$ with totally different scaling factors ζ on the positive and negative side (Fig. 2). At these points the “asymmetric” cycle of the decimation functions observed at ϕ_c has the same length as the “symmetric” one at $\phi = 1/2$.

For all the other points the asymmetry is associated with a constant shift between the wave functions on the positive and negative sides. Numerical iteration of the TBM (1) shows that the wave functions on the positive and negative side are asymptotically related by

$$\psi(F_n) \approx \psi(-F_{n+s}) \quad (7)$$

and the corresponding decimation functions satisfy the equations

$$c_n^+(0) \approx c_{n+s}^-(0), \quad d_n^+(0) \approx d_{n+s}^-(0); \quad (8)$$

i.e., asymptotically there is a shift of s levels between the positive and negative decimation functions. Moreover, in the above $+$ and $-$ can be interchanged with the same shift s , which implies that $c_n^+(0) \approx c_{n+s}^-(0) \approx c_{n+2s}^+(0)$, i.e., the asymptotic period $p = 2s$.

The phenomenon of shifted symmetry helps in locating the limit cycles of period 24 at points *F*, *G*, and the middle point *M* of the line *AC*. With double-precision

arithmetics, the decimation equations can be iterated accurately only about 23 times so that the full asymptotic cycle cannot be seen on one side only. More iterations can be carried out using quadruple precision but at present we cannot go much beyond the 28th decimation level (corresponding to the system size 1 028 455) because of the CPU time limitation. However, even with some initial transients, we can see the asymptotic cycle clearly due to the constant shift between the decimation functions on the positive and negative sides. For all the points *F*, *G*, and *M* the shift s is found to be equal to the period of the symmetric limit cycle appearing at $\phi = 1/2$. Therefore, in these cases the phenomenon of shifted symmetry results in a doubling of the period of a limit cycle for the decimation functions. However, for the point *I* the shift is one-half of the symmetric period so that the asymmetric and the symmetric periods have equal lengths.

Comparison of the limit cycles and the scaling ratios at various points shows that the points *A*, *C*, *M*, *F*, *G*, *H*, *I*, *J*, and *K* define nine new universality classes different from Harper. These quantitative universality classes can be divided into broader qualitative classes of symmetric, asymmetric, and shifted-symmetry wave functions. An example of each case is shown in Fig. 2.

With the exception of the points discussed above (i.e., the points marked by solid circles in the phase diagram), the iteration of the decimation functions in the rest of the *C* phase did not show any limit cycles. Particularly difficult was the study of the *AC* line where the existence of limit cycles at *A*, *C*, and the point *M* was confirmed with the quadruple precision. However, for the rest of the points on this line, the RG iterates came close to the limit cycles of *A*, *C*, and *M* but never converged to any of them [see Fig. 3(a)]. The decimation functions for the lines *AM* and *MC* plotted separately converged on a same invariant set. Analogous results were obtained for the line *CE* where the RG iterates did not converge on a limit cycle except at the points *C*, *K*, and *H* [see Fig. 3(b)]. Furthermore, the iterates of the RG equations for the region bounded by *AC* and *CE* converged on yet another

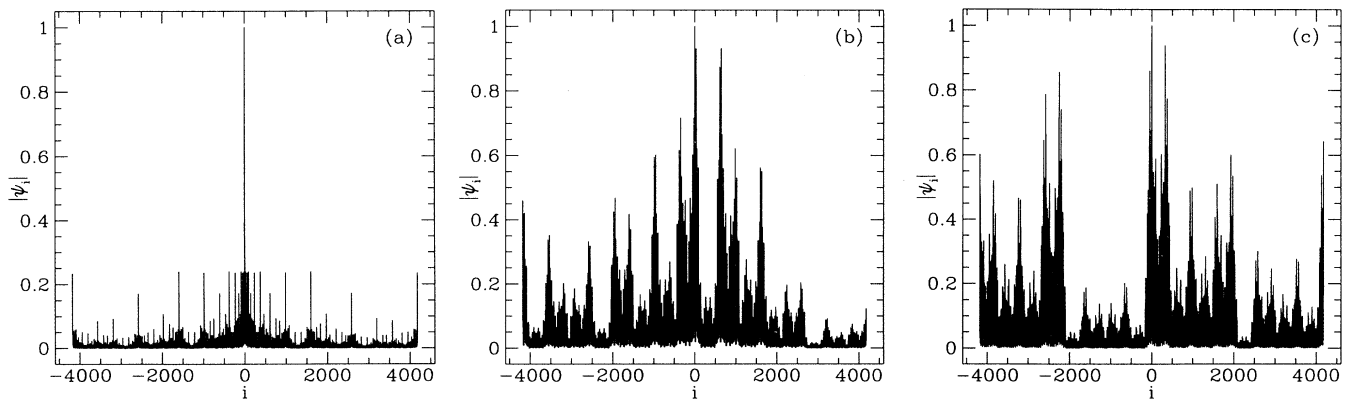


FIG. 2. The absolute value of the wave function at the points *C* (a), *J* (b), and *G* (c) at $E = E_{\min}$. The phase factor ϕ is chosen so that the main peak is centrally located resulting in a bounded wave function (see Table I). (a) is an example of a fully symmetric wave function. (b) is completely asymmetric resulting in different scaling factors on the positive and negative side. (c) is associated with the shifted symmetry where the same ζ 's appear on both sides but the corresponding lattice sites are shifted by a fixed number of decimation levels.

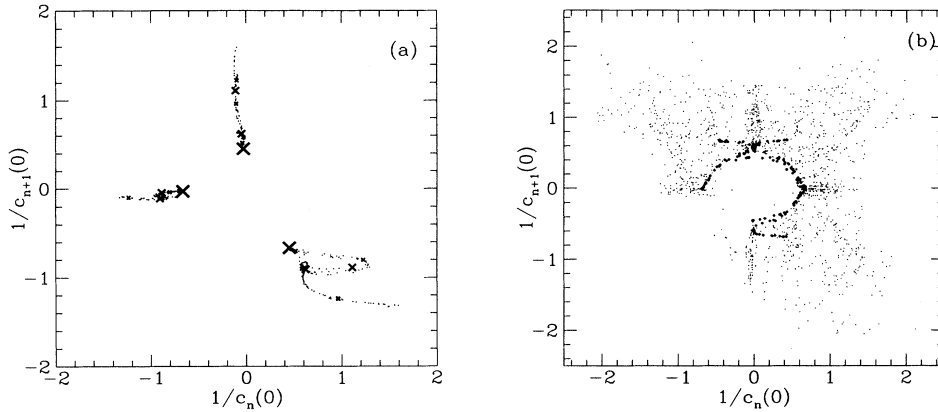


FIG. 3. (a) The inverse decimation function $1/c_n(0)$ vs $1/c_{n+1}(0)$ ($\phi = 1/2$) along the bicritical line AC . The limit cycles for the points M , A , and C are respectively shown by small, medium, and large crosses. (b) Corresponding results for the interior of the critical phase bounded by the AC and CE lines. The dark dots show the data for the CE line, excluding the points C , K , and H .

invariant set which appeared independent of the chosen parameter values at which the decimation equations were iterated. This suggested that the observed behavior was not due to long transients. Although the possibility of limit cycles of order higher than 24 cannot be completely ruled out, we believe that the iterates of AC and CE and the region bounded by them converge on three different invariant sets. It is interesting to note that the invariant set of the CE line encircles the invariant set of the region bounded by AC and CE .

In summary, our decimation scheme conclusively shows that the Bloch electron problem with NNN interactions results in various new universality classes. The wave function corresponding to a band edge is self-similar at isolated points (see Table I) of the phase diagram where the RG flow converges on a limit cycle. Some of these special points were pointed out in a previous study⁸ of the model where they were signaled by periodic oscillations of the TBW superposed on a power law behavior. The previous studies were rather inconclusive in the interior of the critical phase. We show that most of this region can be described by an infinite invariant set of the RG flow. To the best of our knowledge, this is the first example of a quasiperiodic model where the golden mean incommensurability does not result in self-similar wave functions at the band edges. Our studies provide a unique characterization of these fractal states in terms of an invariant bounded set of the RG equations.

A number of open problems remain. (i), we cannot rule out the existence of additional limit cycles in the

critical phase and hence Table I may not be complete. The existence of limit cycles at certain isolated points for which ϕ_c is a rational number (with the exception of point M) suggests that these points may correspond to special symmetries of the TBM. These special characteristics may also explain why the wave functions at certain points are symmetric, asymmetric, or possess the shifted symmetry. (ii), the relationship between the limit cycles of the decimation equations and the periodic oscillations in the TBW (Ref. 8) is not fully understood as seen from Table I. Furthermore, the scaling exponent for the TBW was found to be different on the CD line from the rest of the interior of the C phase. However, for both regions the scaling properties of the wave function seem to be described by the same invariant set. (iii), it would be interesting to linearize the RG operator around some of the new limit cycles using the local form of the operator introduced in Ref. 5.

There have been various attempts to obtain experimental realization⁹ of the critical phase of the Harper model in 2D mesoscopic systems. Calculation of the transport properties in a quantum dot system could provide a possible experimental means to confirm the phase diagram of the generalized Harper model where the critical phase exists in a finite region in parameter space.

The research of I.I.S. is supported by a grant from the National Science Foundation, No. DMR 093296. J.A.K. is grateful for the hospitality during his visit to the George Mason University.

* Present address: Department of Physics, Åbo Akademi, Porthansgatan 3, FIN-20500 Åbo, Finland.

† Electronic address: isatija@sitar.gmu.edu

¹ For a review, see J. B. Sokoloff, Phys. Rep. **126**, 189 (1985).

² P. G. Harper, Proc. Phys. Soc. London A **68**, 874 (1955).

³ S. Ostlund and R. Pandit, Phys. Rev. B **29**, 1394 (1984); S. Ostlund, R. Pandit, D. Rand, H. Schellnhuber, and E. D. Siggia, Phys. Rev. Lett. **50**, 1873 (1983).

⁴ D. J. Thouless and Q. Niu, J. Phys. A **16**, 1911 (1983); R. B. Stinchcombe and S. C. Bell, *ibid.* **20**, L739 (1987); **22**, 7171 (1989); L. Suslov, Sov. Phys. JETP **56**, 612 (1982); **84**, 1972 (1983); **57**, 1044 (1983); M. Wilkinson, J. Phys. A

20, 4357 (1987); C. Wiecek and E. Roman, Phys. Rev. B **30**, 1603 (1984); D. Dominguez, C. Wiecek, and J. V. José, *ibid.* **45**, 13919 (1992).

⁵ J. A. Ketoja and I. I. Satija, Phys. Lett. A **194**, 64 (1994).

⁶ I. I. Satija, Phys. Rev. B **48**, 3511 (1993); **49**, 3391 (1994); I. I. Satija and J. C. Chaves, *ibid.* **49**, 13239 (1994).

⁷ J. A. Ketoja, Phys. Rev. Lett. **69**, 2180 (1992).

⁸ J. H. Han, D. J. Thouless, H. Hiramoto, and M. Kohmoto, Phys. Rev. B **50**, 11365 (1994); Y. Hatsugai and M. Kohmoto, *ibid.* **42**, 8282 (1990).

⁹ R. R. Gerhart, D. Weiss, and K. Von Klitzing, Phys. Rev. Lett. **62**, 1173 (1989).